GEOPHYSICAL RESEARCH LETTERS, VOL. 25, NO.12, PAGES 2189-2192, JUNE 15, 1998

Resonant diurnal internal tides in the North Atlantic

Brian D. Dushaw

Applied Physics Laboratory, College of Ocean and Fisheries Sciences, University of Washington, Seattle

Peter F. Worcester

Scripps Institution of Oceanography, University of California at San Diego, La Jolla

Abstract. Using a large acoustical array located midway between Puerto Rico and Bermuda, we have observed enhanced diurnal tidal signals associated with the lowest internal-wave mode. These signals result from a diurnal internal wave resonantly trapped between the shelf just north of Puerto Rico and the turning latitude, a distance of about 1100 km. The data obtained using the large acoustical array are consistent with the predicted Airy-function variation with latitude of diurnal internal waves near the turning latitude. The existence of this wave is a striking demonstration of the long spatial and temporal coherence of oceanic internal tides. In general, the energy radiated by such waves is a loss of energy from the earth-moon system and a source of energy for mixing in the deep ocean.

Introduction

Tidal currents perturbing the stratification at the boundaries of the ocean basins or at mid-ocean ridges generate internal waves at tidal frequencies. These internal waves radiate into the ocean interior in the form of internal-wave rays [*Rattray et al.* 1969] or, alternatively, modes. Observations of internal tides by long-range acoustical means or satellite altimetry are most sensitive to the signals produced by the lowest mode of excitation in the vertical. Recent observations have shown that waves of the lowest mode can retain coherence far into the ocean's interior [*Hendry* 1977, *Dushaw et al.* 1995, *Ray and Mitchum* 1996]. Such radiation has a turning latitude where its frequency is equal to the inertial frequency [*Hendershott* 1973, *Wunsch and Gill* 1976]; poleward of this latitude these waves cannot propagate freely. Internal waves approaching their turning latitude are refracted back toward the equator. The turning latitude for diurnal frequencies is about 30°. In this paper we discuss observations of internal waves at diurnal frequencies that are resonantly trapped between their turning latitude and the shelf just north of Puerto Rico.

The AMODE Experiment

The 1991–92 Acoustic Mid-Ocean Dynamics Experiment (AMODE) [*The AMODE Group* 1994, *Dushaw et al.* 1998] was a tomographic array consisting of a pentagonal array of moored acoustic transceivers located between Bermuda and Puerto Rico (Figure 1). The ranges between transceiver moorings were about 350, 410, and 660 km.

Paper number 98GL01583.
0094-8534/98/98GL-01583$05.00

The resulting time series of ray travel times covered 180–300 days with sampling occurring every 4 hours on every fourth day. The acoustically-derived barotropic tidal currents were shown to be highly accurate by comparison with a recent global tidal model derived from satellite altimetry [*Dushaw et al.* 1998]. Additional data were obtained from three thermisters located on each tomographic mooring at depths of about 600, 775, and 950 m. All data were high-pass filtered prior to analysis by subtracting daily averages; this filtering does not significantly affect the estimates of diurnal harmonic constants.

In the western North Atlantic, the acoustic eigenrays typically have lower turning depths around 3500 m and upper turning depths around 300 m, and they turn about 20 times over a range of 500 km. A dozen or so rays provide useful oceanographic information. The travel time variations at tidal frequencies observed here are about ± 10 ms, while travel time accuracy is about 1 ms. The acoustic data are corrected for mooring motion using an acoustic navigation system. The tomographic moorings are particularly stiff so the effect of mooring motion on the thermister timeseries is minimized.

Data and Tidal Analysis

The travel times of the acoustic signals are used to determine the amplitude of the first internal wave mode. The acoustic travel times are sensive to sound speed, and the modes in sound speed are obtained by multiplying the displacement modes by the negative of the potential sound speed gradient. The first displacement mode has a maximum at about 1400 m and no zero crossings. The signals of higher-order modes are suppressed in the acoustical data because they have both positive and negative displacements in the vertical [*Dushaw et al.* 1995]. The acoustic ray paths average over the entire water column, and the vertical averages of higher order modes are much smaller than that of the first mode. The mode amplitudes are determined from the travel times using inverse methods which take into account the acoustical ray path sampling [*Munk et al.* 1995]. The maximum first mode displacement at diurnal frequency was found to be about 1 m at a depth of 1400 m, and the maximum temperature variation associated with this displacement is about 0.04°C peak-to-peak at a depth of 800 m. (The normalization of the vertical modes employed here is such that an amplitude of 1 m roughly corresponds to 1 m of displacement at displacement mode maximum [see *Hendry* 1977].)

The thermister data were also used to derive mode amplitudes at the mooring locations. These data do not

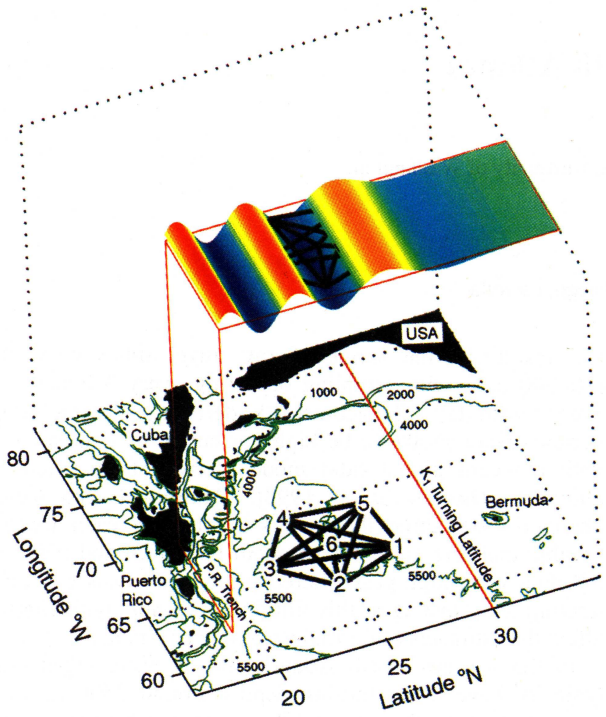

Figure 1. The AMODE acoustic tomography array was located between Puerto Rico and Bermuda. The width of the array was about 670 km and it consisted of six moorings, labeled 1–6. The array detected diurnal signals of the lowest internal wave mode. The predicted horizontal variation of the displacement associated with this mode for the K_1 frequency is shown at the top as the colored wave. The southern boundary is the 600-km long shelf just north of Puerto Rico.

provide the spatial filtering of the acoustic data, but the records are long (350 days) and the three timeseries from each mooring provides some vertical resolution. The first temperature mode was fit to the three thermister time series from each mooring to derive time series of mode amplitude.

The time series of first-mode amplitude were used in a weighted least-squares tidal analysis to determine the harmonic constants for each acoustic path (Figure 2). The time series allow accurate resolution of the tides. The uncertainties in the harmonic constants are about 10% in amplitude and about 10° in phase. The tidal fit using the 8 dominant tidal frequencies accounted for 40–70% of the variance of the acoustic time series. The uncertainties in the thermister results are similar to those in the acoustical results, but the tidal fit accounted for only 7–40% of the variance of the time series. When tidal frequencies are shifted by a value 2π/(record length), the best frequency resolution available, a tidal fit to the acoustical timeseries accounts for only about 8% of the variance, or about the value expected from a time series of random noise. This shows that the acoustically-observed internal tides remain by and large locked to their original tidal frequencies, at least over the available record lengths of 180–300 days. The tidal intermittency frequently observed by point measurements [e.g., *Wunsch* 1975] is apparently not an inherent property of internal tides. All tidal phases here are Greenwich phase.

The dominant diurnal frequencies are the principal solar (K_1, 23.9345 hour period) and principal lunar (O_1, 25.8193 hour period) frequencies. The K_1 and O_1 frequencies have turning latitudes 30.0° and 27.6°, respectively. In the western North Atlantic the surface, or barotropic, tides of these two constituents are comparable in magnitude, and other diurnal frequencies are quite weak. The dominant semidiurnal surface tide, M_2, is an order of magnitude larger than the K_1 or O_1 surface tide. However, the observed diurnal and semidiurnal amplitudes of the internal tide are comparable in size. As will be shown below, the enhanced diurnal amplitude results from resonant trapping of the diurnal internal waves between their turning latitudes and the shelf north of Puerto Rico. Wunsch and Gill [1976] found low-frequency, wind-generated internal waves trapped near the equator by using the statistics of sea-level records from island tide gauges. Wunsch and Gill's result relied on a stochastic description of the variability; the diurnal wave described here is deterministic.

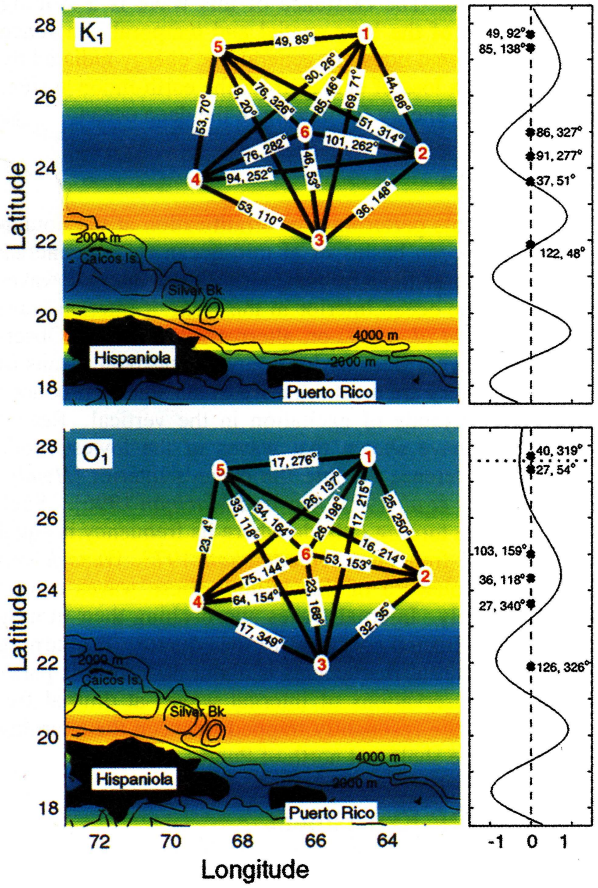

Figure 2. The panels at left show the predicted displacement of diurnal waves at the K_1 and O_1 frequencies, together with the measured harmonic constants for each acoustic path. The panels at right show the predicted displacement as a function of latitude, together with the harmonic constants determined for each mooring from the thermister data. The horizontal dotted line in the panel for O_1 indicates the turning latitude. The boundary condition at 19–20°N is zero meridional flow; this roughly corresponds to a displacement maximum of the K_1 wave.

Theory

The theory of oceanic internal waves near the turning latitude is well known [*Hendershott* 1973, *Wunsch and Gill* 1976]. We derive predictions of the mode-1 K_1 and O_1 waves assuming that the meridional structures of these waves are adequately approximated by Airy functions. The prediction is made without regard to the southern boundary condition (zero meridional flow at Puerto Rico.) The AMODE array is within a few wavelengths of the turning latitude, and the exact latitude of the southern boundary condition is not well defined.

When the variation of inertial frequency with latitude is approximated by a linear function of latitude (the "beta-plane"), meridional current is described by a set of Hermite functions. The scaling constants in these functions are fixed entirely by the relevant parameters: inertial frequency, tidal frequency, and vertical mode eigenvalue. The solutions for the K_1 and O_1 meridional currents on the 25°N beta-plane are described by Hermite functions of order 42 and 36, respectively; the order is determined by the frequency of the variability. These waves have phase speeds of about 7 $m\,s^{-1}$ and group speeds of about 2 $m\,s^{-1}$. The meridional component of group velocity vanishes at the turning latitude. Near the turning latitude, an Airy function approximation to the exact solution is appropriate. The amplitude of the current increases slightly from south to north and decays exponentially north of the turning latitude. The no-flow boundary condition near Puerto Rico is satisfied by chance for the K_1 wave but probably not for the O_1 wave. Because the acoustic data measure sound speed, or temperature, rather than current, the vertical displacement associated with these waves is more relevant. If no zonal variation is assumed, the meridional structure of displacement is proportional to the derivative of the meridional current (Figure 2). Unlike the amplitude of the current, the amplitude of the displacement decreases as the turning latitude is approached from the south.

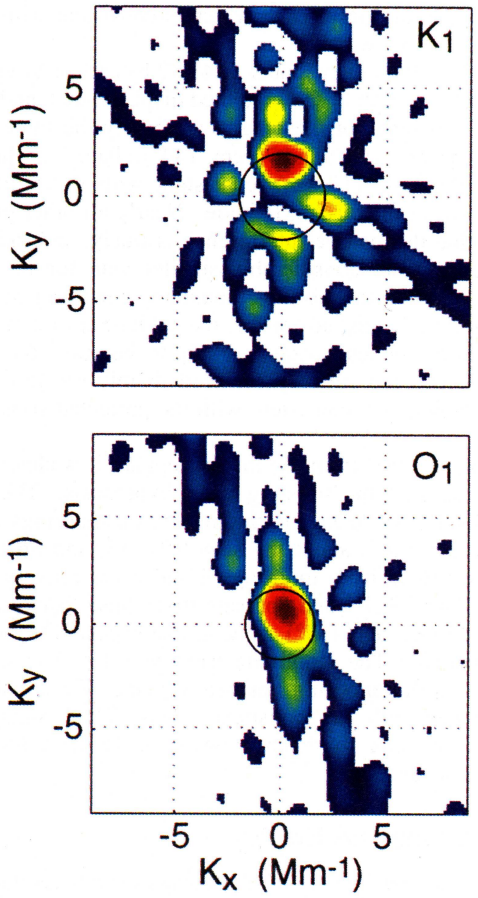

Figure 3. Estimates of the wavenumber spectra for frequencies K_1 and O_1 derived from the tidal harmonic constants of Figure 2. K_x and K_y are zonal and meridional components of the wavenumber, respectively. The circles indicate the approximate magnitude of wavenumbers expected within the AMODE array (wavelengths 488 and 600 km for K_1 and O_1, respectively). The spectrum for K_1 shows a dominant meridional wavenumber, with some weaker peaks. When several waves are present, the spectral estimate can misrepresent the actual wavenumbers present, but the spectra show that predicted and measured wavenumbers agree.

Comparison of Data with Theory

With this theoretical background, we can see how well the data correspond to theory. Beamforming spectral estimates [*Capon* 1969, *Hendry* 1977], modified for line-integral data, determine which wavenumbers are consistent with the harmonic constants found on the various acoustic paths. The spectra estimated for both K_1 and O_1 (Figure 3) are consistent with the theoretical wavenumbers, and these spectral estimates show a dominant meridional wavenumber. For O_1 the turning latitude is within the AMODE array, so the definition of wavenumber is ambiguous. However, we have determined by simulations that the wavenumbers actually present are not well defined by spectral estimation using line-integral data when several waves are present. Thus, the wavenumber spectra do not show the two opposing wavenumber peaks that would be associated with the standing wave predicted by theory, but they do show that the wavenumbers present are consistent with theory.

The harmonic constants are consistent with standing waves, however. For the following discussion the notation "path (1,2)" will indicate the path between mooring 1 and mooring 2. Figure 2 shows the harmonic constants and the geometry of the various acoustic paths. For the K_1 frequency, the paths (2,4), (2,6) and (4,6) all lie along a trough of the predicted displacement, and the amplitudes (94, 101 and 76 cm) and phases (252, 262, and 282°) associated with these paths are consistent with the predicted wave. Path (1,5) has a reduced amplitude (49 cm) and opposite phase (89°); this path is near a node of the standing wave with opposite phase. Paths (1,4), (3,6) and (4,5) have smaller amplitudes (30, 46 and 53 cm) because they span nearly a complete meridional wavelength. Path (1,6) spans only half a wavelength, and it has a large amplitude (85 cm) and opposite phase (46°) compared to paths such as (2,4). The agreement is not perfect, but the spectral estimate suggests that an additional wave propagating to the southwest or northeast is also present. Theoretically, the presence of secondary waves would affect the amplitudes for each path, but the standing wave structure would be retained. The K_1 phases are roughly centered on either

260° or 80°, a bi-phase result which is consistent with the predicted standing wave.

For the O_1 frequency, paths (2,4), (2,6) and (4,6) again all lie along a trough of the predicted displacement, and the harmonic constants for these paths are nearly the same (64 cm, 154°; 53 cm, 153°; and 75 cm, 144°). Path (1,5) has a reduced amplitude (17 cm), consistent with the reduced displacement at the turning latitude. Nearly all other paths are such that destructive interference is likely, and indeed the amplitudes are considerably smaller than for K_1. In addition, because the no-flow boundary condition at the shelf is not well satisfied for O_1, the excitation of a single standing wave in resonance is likely to be less efficient. The O_1 phases are roughly centered mainly on 150°, or 330° in a few cases, consistent with the predicted standing wave.

The data derived from the thermisters are less clear, but generally support the standing wave hypothesis. The K_1 amplitudes derived from the thermisters on moorings 2, 5 and 6 are large and about the same (91, 85, and 86 cm). The phase values from moorings 2 and 6 are roughly the same (277° and 327°) and opposite from those from moorings 1 and 5 (92° and 138°), as would be expected from the predicted wave. The amplitude from mooring 4 is small (37 cm), and this mooring lies near a node. These values roughly agree with the acoustical values. The results for mooring 3 are less consistent, however, and those for O_1 are not consistent.

Tidal Forcing and Energy

The forcing mechanism for these waves is not yet understood. The time of maximum positive internal displacement just north of Puerto Rico corresponds very nearly to the time of maximum offshore barotropic tidal current. Normally upward, or positive, displacement of the stratification would be expected to occur near the maximum onshore current. A further study of the details of the forcing mechanism is required; this mechanism is likely to involve flow both along and across the Puerto Rico Trench. Wunsch and Gill [1976] were able to estimate the Q for the low-frequency internal waves from the width of the spectral peaks of sea level and the fact that wind forcing occurred uniformly over frequencies near the spectral peaks. Because the diurnal internal wave is forced only at a single tidal frequency it is not possible to estimate the Q by line width. If the forcing mechanism of these waves was known, however, it might be possible to estimate the Q from the difference between the forcing phase and the observed phase.

At the K_1 frequency, the ratio of baroclinic energy to barotropic energy is about 29.8 to 15.3 $J m^{-2}$. A similar result is found for the O_1 frequency. Since the baroclinic tide has roughly twice the energy of its barotropic parent, it is evident that energy is stored in the resonating wave. One property of resonance is that more energy is lost from the barotropic tide to internal-wave radiation each tidal cycle than if the internal waves were radiating away freely; this suggests a means by which damping of the barotropic tide may be enhanced in some regions. It is not known how the energy is dissipated from the internal wave, or, equivalently, what mechanism limits the amplitude of the resonance. Related questions are whether the energy is dissipated directly into turbulence in some boundary layer or whether energy loss involves a cascade of energy into higher internal-wave frequencies. These long-standing unanswered questions have a direct relation to the problem of mixing in the deep ocean [*Morozov* 1995, *Munk* 1998].

Acknowledgments. We thank G. & E. Marshall for assistance with data processing and M. Hendershott for suggestions. The Office of Naval Research supported the deployment of the AMODE acoustical array. B.D.D. was supported by the National Science Foundation.

References

The Acoustic Mid-Ocean Dynamics Experiment Group, Moving ship tomography in the North Atlantic, *Eos Trans. AGU*, **75**, 17,21,23, 1994.

Capon, J., High-resolution frequency-wavenumber spectrum analysis, *Proc. IEEE*, **57**, 1408–1418, 1969.

Dushaw, B. D., B. D. Cornuelle, P. F. Worcester, B. M. Howe, and D. S. Luther, Barotropic and baroclinic tides in the central North Pacific Ocean determined from long-range reciprocal acoustic transmissions, *J. Phys. Oceangr.*, **25**, 631–647, 1995.

Dushaw, B. D., G. D. Egbert, P. F. Worcester, B. D. Cornuelle, B. M. Howe, and K. Metzger, A TOPEX/POSEIDON global tidal model (TPXO.2) and barotropic tidal currents determined from long-range acoustic transmissions, *Prog. Oceanogr.*, in press, 1998.

Hendershott, M., Inertial oscillations of tidal period, *Prog. Oceanogr.*, **6**, 1–27, 1973.

Hendry, R. M., Observations of the semidiurnal internal tide in the western North Atlantic ocean, *Phil. Trans. R. Soc. Lond.*, **A286**, 1–24, 1977.

Morozov, E. G., Semidiurnal internal wave global field, *Deep-Sea Res.*, **42**, 135–148, 1995.

Munk, W., Once again: once again - tidal friction, *Prog. Oceanogr.*, in press, 1998.

Munk, W., P. Worcester, and C. Wunsch, *Ocean Acoustic Tomography*, 433 pp., Cambridge Univ. Press, 1995.

Rattray, M. R., J. G. Dworski, and P. E. Kovala, Generation of long internal waves at the continental slope, *Deep-Sea Res.*, **16 Supplement**, 179–195, 1969.

Ray, R. D., and G. T. Mitchum, Surface manifestation of internal tides generated near Hawaii, *Geophys. Res. Lett.*, **23**, 2101–2104, 1996.

Wunsch, C., Internal tides in the ocean, *Rev. Geophys. Space Phys.*, **13**, 167–182, 1975.

Wunsch, C., and A. Gill, Observations of equatorially trapped waves in Pacific sea level variations, *Deep-Sea Res.*, **23**, 371–390, 1976.

B.D. Dushaw, Applied Physics Laboratory, University of Washington, 1013 N.E. 40th St., Seattle, Washington, 98105; dushaw@apl.washington.edu

P.F. Worcester, Scripps Institution of Oceanography, University of California at San Diego, La Jolla, California, 92093-0225; pworcester@ucsd.edu

(received March 2, 1998; accepted April 28, 1998.)